RSC Advances

PAPER

View Article Online
View Journal | View Issue

Cite this: *RSC Adv.*, 2017, **7**, 13433

Microwave assisted synthesis of MoS_2/nitrogen-doped carbon shell–core microspheres for Pt-free dye-sensitized solar cells

Guang Zhu,*[a] Haifeng Xu,[a] Hongyan Wang,[a] Wenqi Wang,[a] Quanxin Zhang,[c] Li Zhang[a] and Hengchao Sun*[b]

Received 30th December 2016
Accepted 24th February 2017

DOI: 10.1039/c6ra28850b

rsc.li/rsc-advances

In this work, novel MoS_2/nitrogen-doped carbon shell–core microspheres (MNCS) have been designed and prepared through the microwave-assisted method, and used as counter electrodes for platinum-free dye-sensitized solar cells (DSSCs). The results show that as-prepared shell–core composite microspheres possess low charge transfer resistance and high electrocatalytic activity. When used as a counter electrode for DSSCs, the powder conversion efficiency of an as-prepared cell with optimized MNCS reaches 6.2% under standard light illumination, which is comparable to cells with a conventional Pt counter electrode.

Introduction

In the development of clean energy, solar energy is a plentiful and environmentally safe energy source. In recent years, dye-sensitized solar cells (DSSCs) have attracted considerable attention as an alternative to conventional silicon based solar cells due to their low cost, easy fabrication and high power conversion efficiency.[1–8] A typical DSSC is composed of a photoanode, an electrolyte, and a counter electrode. Among them, the counter electrode (CE) reduces the oxidized electrolyte, which is critical for high performance DSSCs.[9–12] So far, platinum is still the most widely-used CE for DSSCs due to its excellent electrical conductivity and high catalytic activity.[13–20] However, the use of noble Pt metal would be limited by the scarcity and high cost. Therefore, it is necessary to explore the low cost and Pt-free CEs to facilitate the industrial development of DSSCs.

As a typical layered transition metal sulfide, molybdenum disulfide (MoS_2) has attracted considerable attention and was proposed as an effective candidate counter electrode to replace Pt for DSSCs due to its analogous structure to graphene.[21,22] However, the drawback of MoS_2 is that its active sites are limited to its edges, which decreases the DSSC's performance.[23–26] Recently, some works have demonstrated that MoS_2 incorporated with carbon composites could lower the charge transfer resistance and enhance the electrocatalytic activity, which can improve the photovoltaic performance.[27–31] Tai *et al.* prepared multi-walled carbon nanotubes (MWCNTs) and MoS_2 nanocomposites as counter electrodes for DSSCs, and a conversion efficiency of 6.41% was obtained.[32] Liu *et al.* prepared MoS_2 and graphene composite by simply mixing graphene oxide nanosheets with MoS_2 as counter electrodes and a conversion efficiency of 6.04% was achieved.[33] Yue *et al.* fabricated MoS_2/carbonaceous hybrid material by a hydrothermal route as CE materials for DSSCs, and showed a photovoltaic efficiency of 7.69%.[34] Despite the above process has been achieved, the design and fabrication of MoS_2 incorporated with carbon material composites with high electrocatalytic activity for DSSCs are still very challenging.

In our previous work, the nitrogen-doped carbon microspheres (NCS) were prepared *via* a simple, rapid and effective microwave assisted method and used as CEs for DSSCs. To further expand the application of this method in DSSCs, herein we report the fabrication of novel MoS_2/nitrogen-doped carbon shell–core microspheres (MNCS) *via* all microwave assisted method for DSSCs. To our knowledge, there are rare research reports on enhanced photovoltaic performance of DSSCs based on the type of MoS_2/nitrogen-doped carbon shell–core microspheres CEs. It is found that as-prepared MNCS can lower the charge transfer resistance and enhance the electrocatalytic activity. When it serves as the CEs in DSSCs, a high conversion efficiency of 6.2% can be achieved under one sun illumination, which is comparable to the cell with conventional Pt counter electrode.

Experimental

NCS was fabricated *via* the microwave-assisted method reported in our previous work.[35] Subsequently, the MNCS was fabricated

[a]*Anhui Key Laboratory of Spin Electron and Nanomaterials, Suzhou University, Suzhou 234000, P. R. China. E-mail: guangzhu@ahsztc.edu.cn; Fax: +86-557-2871003; Tel: +86-557-2871006*

[b]*Institute of Microelectronics, Chinese Academy of Science, Beijing 100029, P. R. China. E-mail: sunhengchao@ime.ac.cn*

[c]*Lanzhou Institute of Chemical Physics, Chinese Academy of Sciences, Lanzhou 730000, P. R. China*

via microwave-assisted method again. In brief, the appropriate amount of as-prepared NCS was dissolved in 100 ml of 20 mM trioxomolybdenum-phosphoric solution, and then followed by ultrasonication for 30 min. And then, 100 ml of 70 mM thioacetamide was added into the reaction solution under stirring. After that, the above solution was heated at 160 °C with a microwave irradiation power of 100 W for 10 min using a microwave system (Explorer-48, CEM Co.). After being centrifuged and washed with deionized water, the resultant precipitate was dried in a vacuum oven at 120 °C for 12 h, and finally thermally treated at 800 °C for 2 h in an ammonia atmosphere. In this work, the amount of NCS was set as 53.3 mg, 80 mg, and 160 mg, and the corresponding obtained samples are denoted as MNCS-1, MNCS-2, and MNCS-3, respectively. The MNCS counter electrode was prepared by drop coating method on the cleaned F-doped SnO_2 (FTO) glass. In addition, the pure MoS_2 and conventional Pt counter electrodes were prepared for comparison. The DSSCs devices with the active area of 0.2 cm^2 were assembled and fabricated based on our previous work.[35]

The surface morphologies of the samples were measured by the JEOL JSM-LV5610 field emission scanning electron microscopy (FESEM) and JEOL-2010 high-resolution transmission electron microscopy (HRTEM), respectively. Nitrogen adsorption–desorption isotherms were measured at 77 K with an ASAP 2020 Accelerated Surface Area and Porosimetry System (Micrometitics, Norcross, GA). The compositions of the samples were analyzed by a Holland Panalytical PRO PW3040/60 X-ray diffraction (XRD) with Cu Kα radiation (V = 30 kV, I = 25 mA). Cyclic voltammetry (CV) measurements were carried out by an electrochemical workstation (Autolab PGSTAT 302N) in a three electrode electrochemical system, which contained an ACN solution of 10 mM LiI, 1.0 mM I_2, and 0.1 M $LiClO_4$. Electrochemical impedance spectroscopy (EIS) measurements were performed by the above mentioned electrochemical workstation under 100 mW cm^{-2} illumination at an applied bias of V_{oc}, applying a 10 mV AC sinusoidal signal over the constant applied bias with the frequency ranging between 100 kHz and 0.1 Hz. The performance of as-prepared devices was measured by a Newport solar simulator fitted with an AM 1.5 G filter, in conjunction with a Keithley 2440 source meter.

Results and discussion

The morphologies of the as-prepared NCS and MNCS were investigated by FESEM. Fig. 1a shows the morphology of the as-prepared NCS. It can be observed that these nitrogen-doped carbon microspheres are quite uniform and monodispersed, with an average diameter of around 2 μm. Compared with pure nitrogen-doped carbon microspheres, a out-layer of MoS_2 with a thickness of *ca.* 200 nm can be observed on the surface of microspheres. The results indicate that the shell–core structured MoS_2/nitrogen-doped carbon microspheres were fabricated *via* microwave assisted method. Fig. 2 shows the HRTEM image of as-prepared MNCS. The lattice from MoS_2 outlayer can observed clearly. The interlayer spacing of 0.62 nm observed

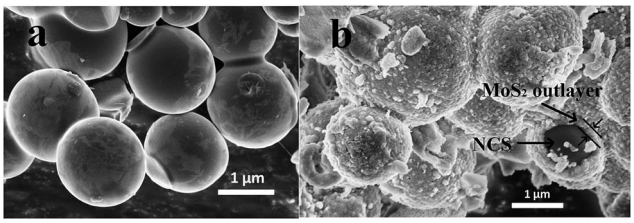

Fig. 1 FESEM images of the as-prepared (a) nitrogen-doped carbon microspheres and (b) MoS_2/nitrogen-doped carbon shell–core microspheres.

from lattice fringes can be ascribed to the (002) direction of hexagonal MoS_2

Fig. 3 shows the N_2 adsorption–desorption isotherms of as-prepared MoS_2 and MNCS-2. The Brunauer–Emmet–Teller (BET) specific surface area and mean pore diameter were determined and summarized in Table 1. As seen, the MNCS-2 shows a higher BET specific surface area (35.39 m^2 g^{-1}) and larger pore volume (16.02 nm) than MoS_2 (2.64 m^2 g^{-1} and 9.52 nm), respectively. The greatly enhanced specific surface area provides more active plots to reduce I_3^-.

The phase structure of the as-synthesized pure MOS_2 and MNCS composites with different NCS amounts was further characterized by using XRD. As shown in Fig. 4, all samples exhibit a hexagonal MoS_2 crystal structure (JCPDS 75-1539). Moreover, the strong (002) diffraction peak at 14.4° can be observed in samples, indicating a well stacked layered structure of MOS_2.[36] The broad peaks at 24° corresponds to (002) diffraction mode of graphitic structure, which is characteristic of disordered carbon material.[37,38] It is noted that the (002) diffraction peak gradually becomes weak with the decrease of NCS amount. The results further confirm that MoS_2/nitrogen-doped carbon composite microspheres can be fabricated *via* this method.

CV measurements were carried out to analyze the electrochemical catalytic activity of as-prepared electrodes. Fig. 5 indicates the CV curves of the pure MoS_2, various MNCSs and Pt counter electrodes under the potential from −0.5 to 1.2 V for the I_3^-/I^- redox couple. Two pairs of oxidation and

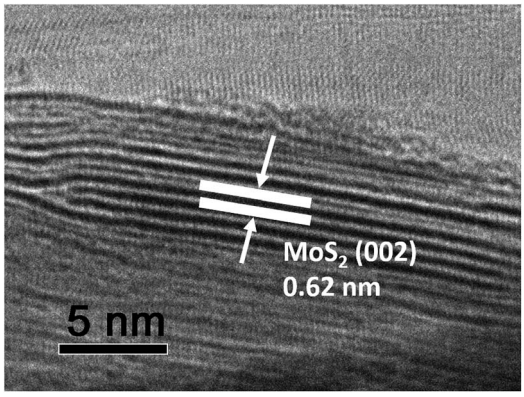

Fig. 2 The HRTEM image of as-prepared MoS_2/nitrogen-doped carbon shell–core microspheres.

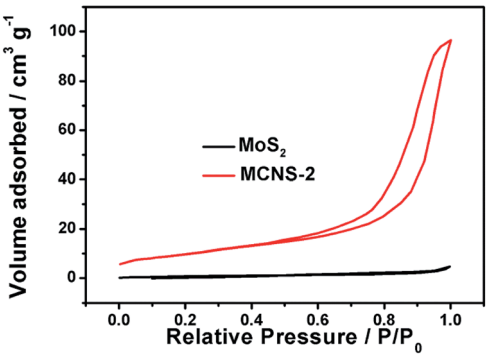

Fig. 3 Nitrogen adsorption–desorption isotherms of as-prepared MoS_2 and MNCS-2.

Table 1 Specific surface area and mean pore diameter of as-prepared MoS_2 and MCNS-2

Sample	Specific surface area/m^2 g^{-1}	Mean pore diameter/nm
MoS_2	2.64	9.52
MNCS-2	35.39	16.02

reduction peaks are observed, which are assigned to the following reactions.[39,40]

$$3I^- \leftrightarrow I_3^- + 2e^- \quad (1)$$

$$2I_3^- \leftrightarrow 3I_2 + 2e^- \quad (2)$$

The peak positions of the CV curves for as-prepared MNCS electrodes are similar to that of Pt, indicating that MNCS electrodes have a similar electrocatalytic function for the redox reaction to Pt electrode. Among these electrodes, MNCS-2 indicates higher current density than other electrodes based on MoS_2, which could be due to the larger specific surface area and higher reactivity in MCNS-2 electrode for catalysis.[41]

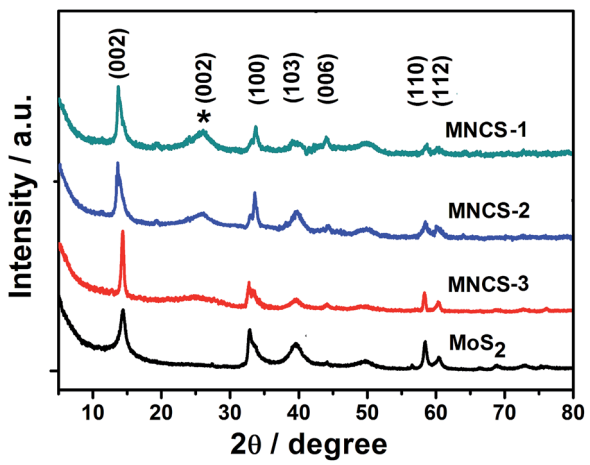

Fig. 4 XRD patterns of as-prepared pure MOS_2 and MNCS composites.

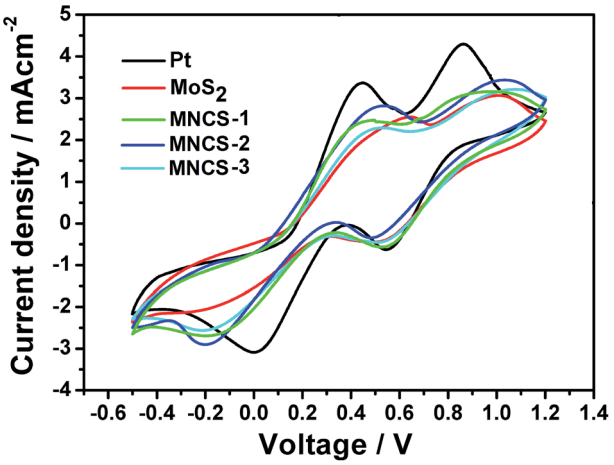

Fig. 5 CV curves of the pure MoS_2, various MNCSs and Pt counter electrodes.

Fig. 6 displays the typical EIS spectra of the cells with various counter electrodes. Two semicircles, including a large one at high frequency and a small one at low frequency, can be observed in the Nyquist plots of EIS spectra. The left semicircle at high frequency represents the charge-transfer resistance (R_{CT}) and the corresponding capacitance (CPE_1) at the interface of the electrolyte/counter electrode. The right semicircle at low frequency represents the charge-transfer resistance (R_w) and corresponding capacitance (CPE_2) at the TiO_2/dye/electrolyte interface.[42] As listed in Table 2, the fitted R_{CT} values of pure MoS_2, MNCS-1 and MNCS-3 CEs are 20.1, 8.8 and 7.8 Ω, respectively. However, as for the MNCS-2 CE (6.1 Ω) is lower than that of Pt CE (7.2 Ω), indicating its high electrocatalytic performance. The low R_{CT} value indicates superior electrocatalytic activity for I_3^- reduction, which is beneficial to the fill factor and conversion efficiency.

The *J–V* curves of DSSCs with various CEs were measured under one sun illumination (100 mW cm^{-2}, AM 1.5 G) and showed in Fig. 7. The corresponding photovoltaic parameters, such as the open circuit potential (V_{oc}), short circuit current density (J_{sc}), fill factor (FF), and conversion efficiency (η) are

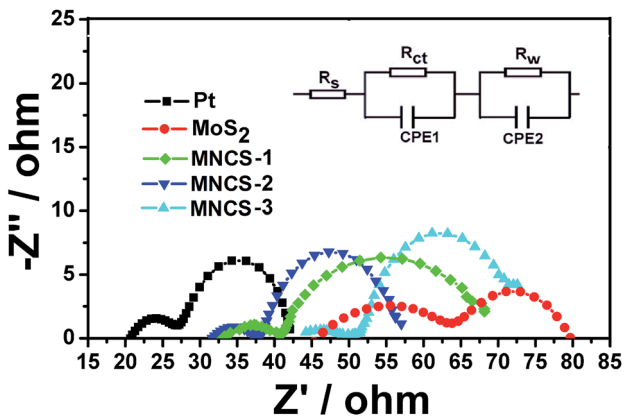

Fig. 6 EIS spectra of the pure MoS_2, various MNCSs and Pt counter electrodes, the inset is the corresponding equivalent circuit.

Table 2 Photovoltaic parameters of the cells with various counter electrodes

Sample	R_{CT}/Ω	J_{sc}/mA cm^{-2}	V_{oc}/V	FF/%	η/%
Pt	7.2	14.9	0.72	65.2	7.0
MoS_2	20.1	13.6	0.72	50.8	5.0
MNCS-1	8.8	14.0	0.71	60.2	6.0
MNCS-2	6.1	14.2	0.71	61.3	6.2
MNCS-3	7.8	13.8	0.71	56.2	5.5

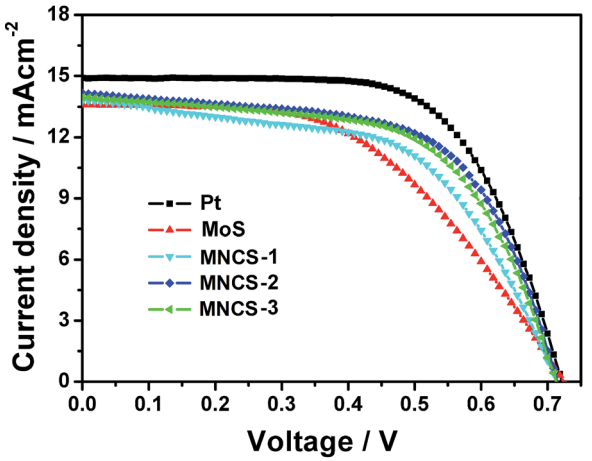

Fig. 7 *J*–*V* curves of DSSCs with various CEs.

listed in Table 2. The J_{sc} and FF of the cell with pure MoS_2 are 13.6 mA cm^{-2} and 50.8%, respectively, resulting in a low conversion efficiency of 5.0%. When nitrogen-doped carbon microspheres are introduced, J_{sc}, FF and η increase obviously and reach maximum values of 14.20 mA cm^{-2}, 61.3% and 6.2% for the cell with MNCS-2 CE, which is due to the high electrocatalytic activity and low charge transfer resistance resulting from the interaction between nitrogen-doped carbon microspheres and MoS_2. However, conversion efficiency will decreases with a further increase of nitrogen-doped carbon microspheres amount, which is ascribed to reduced electrocatalytic activity resulting from the excessive nitrogen-doped carbon microspheres. Despite the maximum η of 6.2% for the cell with MNCS-2 CE is lower than that of Pt CE (7.0%). However, considering the low cost and superior chemical stability of MNCS composites, the MNCS CEs are still competitive to conventional Pt CE.

Conclusion

In summary, MoS_2/nitrogen-doped carbon shell–core microspheres have been synthesized through a microwave-assisted method and used as a Pt-free counter electrode in DSSCs. The results indicate that as-prepared composite counter electrodes exhibit high electrocatalytic activity and low charge transfer resistance resulting from the interaction between nitrogen-doped carbon microspheres and MoS_2. Under optimal conditions, a maximum photovoltaic conversion efficiency of 6.2% under one sun illumination is achieved for DSSCs with MNCS-2 CE, which is comparable to that for conventional Pt counter electrode. That suggests that as-prepared MNCS composite CEs show great potential as a low cost alternative to Pt for DSSCs.

Acknowledgements

This work is supported by the Provincial Natural Science Foundation of Anhui (1508085ME104), the National Science Foundation of China (NSFC) (51602430), the Important Project of Anhui Provincial Education Department (KJ2015A250 and KJ2016A889), the Key Program of Outstanding Youth Talents in Higher Education Institution (GXYQZD2016343), the Program of Innovative Research Team of Anhui Provincial Education Department (Photoelectric information materials and new energy devices).

Notes and references

1 M. Gratzel, *Nature*, 2001, **414**, 338.
2 C. Zha, L. Shen, X. Zhang, Y. Wang, B. A. Korgel, A. Gupta and N. Bao, *ACS Appl. Mater. Interfaces*, 2013, **6**, 122.
3 X. Huang, D. Qin, X. Zhang, Y. Luo, S. Huang, D. Li and Q. Meng, *RSC Adv.*, 2013, **3**, 6922.
4 G. Zhu, L. K. Pan, T. Lu, T. Xu and Z. Sun, *J. Mater. Chem.*, 2011, **21**, 14869.
5 H. Chen, D. Kou, Z. Chang, W. Zhou, Z. Zhou and S. Wu, *ACS Appl. Mater. Interfaces*, 2014, **6**, 20664.
6 D. S. Yang, C. Kim, M. Y. Song, H. Y. Park, J. C. Kim, J. J. Lee, M. J. Ju and J. S. Yu, *J. Phys. Chem. C*, 2014, **118**, 16694.
7 H. Sun, D. Qin, S. Huang, X. Guo, D. Li, Y. Luo and Q. Meng, *Energy Environ. Sci.*, 2011, **4**, 2630.
8 X. J. Sang, J. S. Li, L. C. Zhang, Z. M. Zhu, W. L. Chen, Y. G. Li, Z. M. Su and E. B. Wang, *Chem. Commun.*, 2014, **50**, 14678.
9 R. Jia, J. Chen, J. Zhao, J. Zheng, C. Song, L. Li and Z. Zhu, *J. Mater. Chem.*, 2010, **20**, 10829.
10 S. Hou, X. Cai, H. Wu, X. Yu, M. Peng, K. Yan and D. Zou, *Energy Environ. Sci.*, 2013, **6**, 3356.
11 Y. Xue, J. Liu, H. Chen, R. Wang, D. Li, J. Qu and L. Dai, *Angew. Chem., Int. Ed.*, 2012, **51**, 12124.
12 L. Song, Q. Luo, F. Zhao, Y. Li, H. Lin, L. Qu and Z. Zhang, *Phys. Chem. Chem. Phys.*, 2014, **16**, 21820.
13 M. Tathavadekar, M. Biswal, S. Agarkar, L. Giribabu and S. Ogale, *Electrochim. Acta*, 2014, **123**, 248.
14 M. Wu, X. Lin, T. Wang, J. Qiu and T. Ma, *Energy Environ. Sci.*, 2011, **4**, 2308.
15 S. Pan, Z. Yang, P. Chen, X. Fang, G. Guan, Z. Zhang, J. Deng and H. Peng, *J. Phys. Chem. C*, 2014, **118**, 16419.
16 M. Y. Yen, C. K. Hsieh, C. C. Teng, M. C. Hsiao, P. I. Liu, C. C. M. Ma, M. C. Tsai, C. H. Tsai, Y. R. Lin and T. Y. Chou, *RSC Adv.*, 2012, **2**, 2725.
17 H. C. Sun, T. Q. Chen, Y. Liu, X. Hou, L. Zhang, G. Zhu, Z. Sun and L. K. Pan, *J. Colloid Interface Sci.*, 2015, **445**, 326.
18 Y. Bai, X. Zong, H. Yu, Z. G. Chen and L. Wang, *Chem.–Eur. J.*, 2014, **20**, 8670.
19 M. Wu, X. Lin, Y. Wang, L. Wang, W. Guo, D. Qi, X. Peng, A. Hagfeldt, M. Gratzel and T. Ma, *J. Am. Chem. Soc.*, 2012, **134**, 3419.

20 F. Gong, H. Wang, X. Xu, G. Zhou and Z. S. Wang, *J. Am. Chem. Soc.*, 2012, **134**, 10953.
21 S. Hussain, S. F. Shaikh, D. Vikraman, R. S. Mane, O.-S. Joo, M. Naushad and J. Jung, *ChemPhysChem*, 2015, **16**, 3959.
22 A. Antonelou, G. Syrrokostas, L. Sygellou, G. Leftheriotis, V. Dracopoulos and S. N. Yannopoulos, *Nanotechnology*, 2016, **27**, 045404.
23 L. Sanchez, D. Lembke, M. Kayci, A. Radenovic and A. Kis, *Nat. Nanotechnol.*, 2013, **8**, 497.
24 Q. Xiang, J. Yu and M. Jaroniec, *J. Am. Chem. Soc.*, 2012, **134**, 6575.
25 R. Ganatra and Q. Zhang, *ACS Nano*, 2014, **8**, 4074.
26 M. L. Tsai, S. H. Su, J. K. Chang, D. S. Tsai, C. H. Chen, C. I. Wu, L. J. Li, L. J. Chen and J. H. He, *ACS Nano*, 2014, **8**, 8317.
27 Z. Chen, A. J. Forman and T. F. Jaramillo, *J. Phys. Chem. C*, 2013, **117**, 9713.
28 G. T. Yue, J. Y. Lin, S. Y. Tai, Y. Xiao and J. H. Wu, *Electrochim. Acta*, 2012, **85**, 162.
29 Y. J. Tang, Y. Wang, X. L. Wang, S. L. Li, W. Huang, L. Z. Dong, C. H. Liu, Y. F. Li and Y. Q. Lan, *Adv. Energy Mater.*, 2016, **6**, 1600116.
30 S. A. Patil, P. Y. Kalode, R. S. Mane, D. V. Shinde, A. Doyoung, C. Keumnam, M. M. Sung, S. B. Ambade and S. H. Han, *Dalton Trans.*, 2014, **43**, 5256.
31 W. Wei, K. Sun and Y. H. Hu, *J. Mater. Chem. A*, 2016, **4**, 12398.
32 S. Y. Tai, C. J. Liu, S. W. Chou, F. S. Chien, J. Y. Lin and T. W. Lin, *J. Mater. Chem.*, 2012, **22**, 24753.
33 C. J. Liu, S. Y. Tai, S. W. Chou, Y. C. Yu, K. D. Chang, S. Wang, F. S. Chien, J. Y. Lin and T. W. Lin, *J. Mater. Chem.*, 2012, **22**, 21057.
34 G. T. Yue, J. H. Wu, Y. M. Xiao, M. L. Huang, J. M. Lin and J. Y. Lin, *J. Mater. Chem. A*, 2013, **1**, 1495.
35 G. Zhu, H. Y. Wang, H. Xu, Q. Zhang, H. Sun and L. Zhang, *RSC Adv.*, 2016, **6**, 58064.
36 Z. Wu, B. Fang, Z. Wang, C. Wan, Z. Liu, F. Liu, W. Wang, A. Alfantazi, D. Wang and D. P. Wilkinson, *ACS Catal.*, 2013, **3**, 2101.
37 T. Q. Chen, L. K. Pan, T. Loh, Y. F. Yao, Q. Chen, D. S. Li, W. Qin and Z. Sun, *Dalton Trans.*, 2014, **43**, 14931.
38 T. Q. Chen, L. K. Pan, X. J. Liu and Z. Sun, *Mater. Chem. Phys.*, 2013, **142**, 345.
39 G. Boschloo and A. Hagfeldt, *Acc. Chem. Res.*, 2009, **42**, 1819.
40 J. D. Roy Mayhew, D. J. Bozym, C. Punckt and I. A. Aksay, *ACS Nano*, 2010, **4**, 6203.
41 P. Li, J. Wu, J. Lin, M. Huang, Y. Huang and Q. Li, *Sol. Energy*, 2009, **83**, 845.
42 G. Zhu, L. K. Pan, H. C. Sun, X. J. Liu, T. Lv, T. Lu, J. Yang and Z. Sun, *ChemPhysChem*, 2012, **13**, 769.